

<sup>1</sup>  
<sup>2</sup> Delayed introduction and susceptible variation drive spatial  
<sup>3</sup> asynchrony in pertussis epidemics

<sup>4</sup>  
<sup>5</sup> Sang Woo Park<sup>1,\*</sup>

<sup>6</sup> **1** School of Biological Sciences, Seoul National University, Seoul, Korea

<sup>7</sup> \*Corresponding author: sangwoopark@snu.ac.kr

## <sup>8</sup> **Abstract**

<sup>9</sup> Infectious disease outbreaks typically exhibit a large-scale, spatial synchrony, re-  
<sup>10</sup> flecting coupling through shared environmental forcing and human mobility. Dur-  
<sup>11</sup> ing South Korea's unprecedented large pertussis outbreak in 2024—2025, however,  
<sup>12</sup> asynchronous epidemic patterns were observed throughout the country: some regions  
<sup>13</sup> experienced two epidemic waves, while others regions experienced only the first or  
<sup>14</sup> second wave. Using high-resolution surveillance data from 252 municipalities and a  
<sup>15</sup> simple transmission model, we show that heterogeneity in introduction timing and  
<sup>16</sup> local susceptibility can drive such fine-scale asynchrony even when transmission is  
<sup>17</sup> spatially homogeneous. These results redefine epidemic synchrony as a condition  
<sup>18</sup> contingent not only on shared transmission dynamics, but also on variation in initial  
<sup>19</sup> epidemic conditions.

20 Spatiotemporal variation in epidemic dynamics offers a powerful means for un-  
21 derstanding factors that determine the timing and magnitude of epidemic waves  
22 across populations [1, 2, 3, 4]. Ecological theory predicts that spatial coupling—via  
23 shared environmental forcing and human mobility—can synchronize epidemic dy-  
24 namics between neighboring locations, sometimes manifesting as travelling waves,  
25 where epidemic waves propagate through space [5, 6, 7]. Consistent with this theory,  
26 large-scale spatial synchrony has been observed across diverse pathogens, including  
27 measles [7], dengue [8], influenza [9], RSV [4], and SARS-CoV-2 [10], highlighting  
28 the ubiquity of spatial coupling in shaping epidemic dynamics.

29 Between 2024 and 2025, an unprecedented large pertussis outbreak occurred in  
30 Korea, resulting in more than 50,000 cases by early 2025 (Figure 1) [11]. This out-  
31 break marked a dramatic increase in the disease compared to 292 cases reported in  
32 2023 and 21 cases reported in 2022, despite high vaccine coverage (91.1% of identified  
33 2024 cases had a known vaccination history) [12, 11]. The outbreak consisted of two  
34 waves that peaked around late July and December 2024 (Figure 1A) and exhibited  
35 large spatial heterogeneity in timing (Figure 1B,C) and magnitude (Figure 1D). For  
36 example, both Seoul, the capital city located in the northwest region, and Busan,  
37 the second most populated city located at the southeast end, experienced two waves,  
38 whereas Daegu, the fourth most populated city located < 100km away from Busan,  
39 only experienced the second wave (Figure 1C; see Figure S1 for epidemic dynam-  
40 ics in other regions). This pronounced asynchrony deviates from our expectations  
41 based on spatial coupling, raising questions about mechanisms driving this fine-scale  
42 spatiotemporal heterogeneity in pertussis epidemic [13].

43 To address this question, we combine a detailed spatiotemporal surveillance data  
44 from 252 municipalities in Korea (Figure 1) with mathematical modeling approaches.  
45 We begin by showing that asynchrony in pertussis epidemics, captured by heteroge-  
46 neous epidemic timing, is associated with differences in introduction delays. In con-  
47 trast, the analysis of transmission dynamics reveals synchrony in underlying trans-  
48 mission patterns. Integrating these findings into a mathematical model illustrates  
49 that the apparent asynchrony can be explained by differences in initial epidemic  
50 conditions (i.e., introduction delays and initial susceptibility).

## 51 **Asynchrony in pertussis epidemics associated with introduc- 52 tion delays**

53 First, to characterize spatial heterogeneity in pertussis waves across Korea, we quan-  
54 tify the center of gravity (Figure 1E), which represents the mean timing of cases  
55 [1]. Notably, we find a sharp contrast between early (orange) and late (light blue)  
56 waves between many neighboring municipalities (Figure 1E), suggesting spatial asyn-  
57 chrony in pertussis dynamics. To systematically evaluate this apparent asynchrony,  
58 we estimated the spatial synchrony function, which captures changes in correlation  
59 in epidemic dynamics as a function of distance [7]. The spatial synchrony func-  
60 tion confirms a sharp reduction in cross-correlation with distance (Figure 1F). For

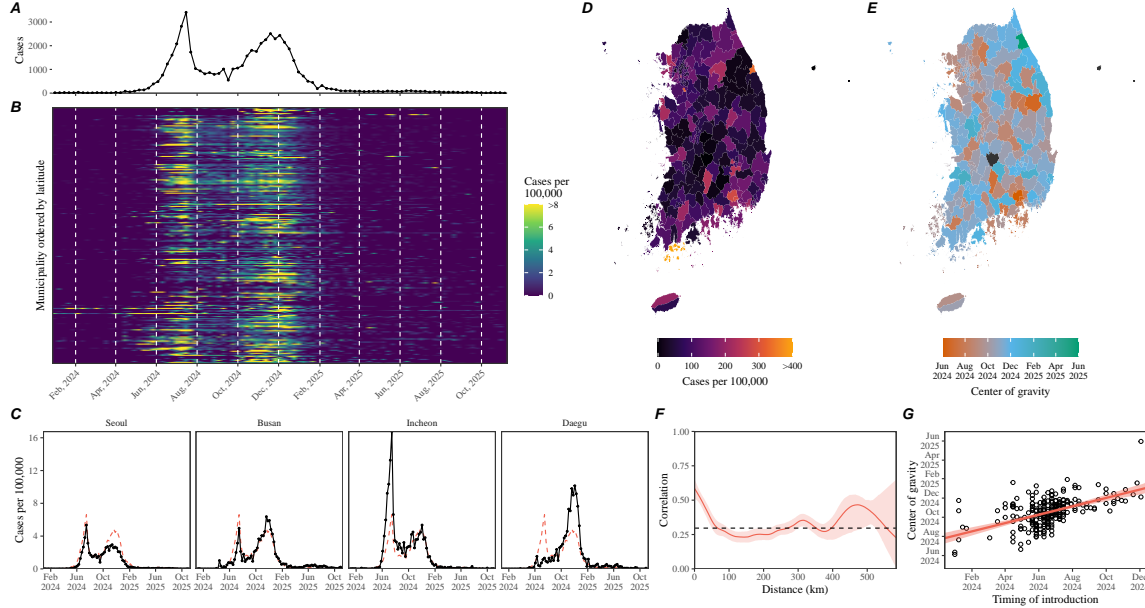
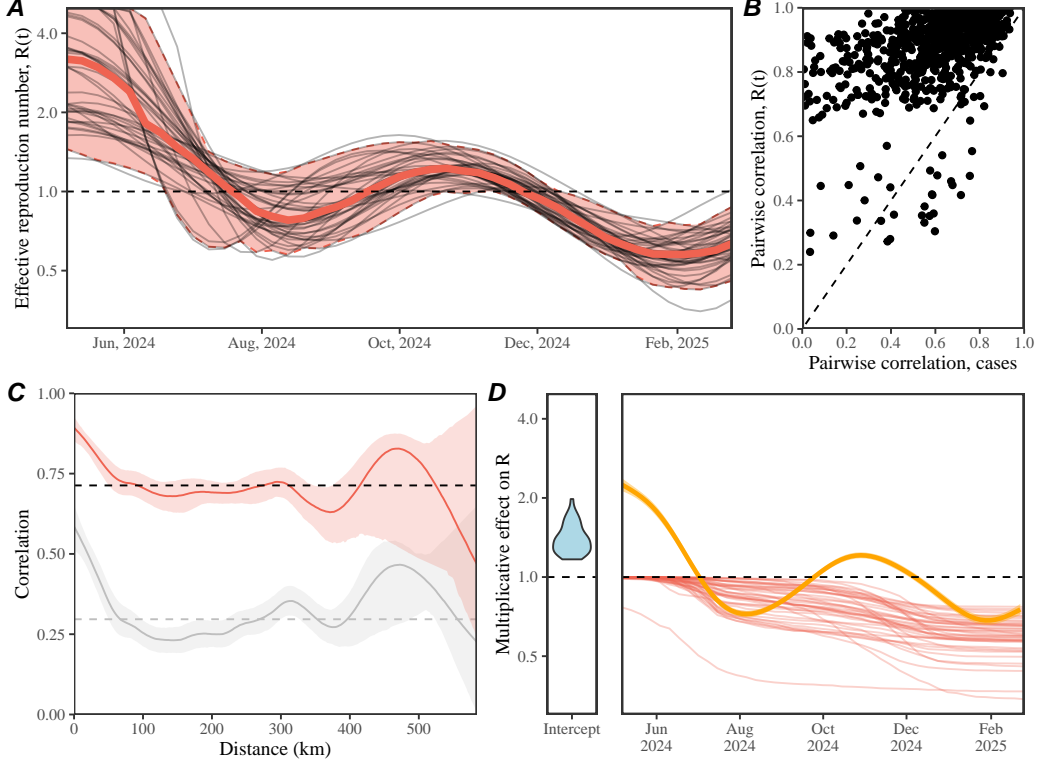


Figure 1: **Spatiotemporal dynamics of pertussis outbreak in Korea, 2024–2025.** (A) Total number of reported cases in Korea. (B) Number of reported cases per 100,000 individuals by municipality, ordered by latitude. (C) Number of reported cases per 100,000 individuals in four most populated cities in Korea. (D) Map of pertussis cases per 100,000 individuals between January 2024 and November 2025. (E) Map of center of gravity, which represents the mean timing of cases. (F) Spatial synchrony in logged cases as a function of distance. The red solid line and shaded regions represent the median estimate and the corresponding 95% confidence interval. The dashed horizontal line represents the mean correlation. (G) Relationship between center of gravity and the timing of introduction, defined as the first week when the number of reported cases is greater than 1 in 100,000. The red solid line and shaded regions represent the linear regression fit and the corresponding 95% confidence interval.

example, within 100km of distance, the cross-correlation drops below 0.25. By comparison, pertussis epidemics in the US maintained cross-correlations above 0.2 even at 1,000 km [14], highlighting the fine-scale asynchrony in pertussis epidemics in Korea. Interestingly, the variation in the center of gravity significantly correlates with the introduction timing ( $\rho = 0.53$ ; 95%CI: 0.44–0.62; Figure 1G), suggesting that differences in introduction timing may contribute to the apparent spatial asynchrony.

## 67 Synchrony in temporal changes in pertussis transmission

We then ask whether the observed epidemic asynchrony can be explained by the differences in transmission patterns. To do so, we quantify the effective reproduction number  $\mathcal{R}(t)$ , which measures the average number of new infections caused by a



**Figure 2: Spatial variation in the estimates of effective reproduction number.** (A) Each black line represents the estimated effective reproduction number for a given municipality with more than 400 total cases. The red solid line and shaded regions represent the median and 95% quantiles of effective reproduction number estimates. (B) Relationship between correlation coefficient for  $\mathcal{R}(t)$  and correlation coefficient for reported cases across all pairwise municipality combinations with more than 400 total cases. (C) Spatial synchrony in  $\mathcal{R}(t)$  (red) versus logged cases (black) as a function of distance. The solid line and shaded regions represent the median estimate and the corresponding 95% confidence interval. The dashed horizontal line represents the mean correlation. (D) Estimated multiplicative effects on  $\mathcal{R}(t)$  from the regression analysis. The blue shaded violin represents the distribution of intercept effect, where a separate intercept term is estimated for each municipality. The red lines represent the estimated susceptible depletion effect for each municipality. The orange line and shaded regions represent the estimated changes in transmission from a smooth term and the corresponding 95% confidence interval.

71 single infected individual [15, 16]. For this analysis, we focus on municipalities with  
 72 more than 400 total cases reported because  $\mathcal{R}(t)$  estimates can be unstable when the  
 73 number of infections are low.

74 Notably,  $\mathcal{R}(t)$  estimates appear to be largely homogeneous across different re-  
 75 gions, despite the apparent heterogeneity in the observed epidemic dynamics (Figure  
 76 2A). Comparisons of correlation coefficients in  $\mathcal{R}(t)$  versus correlation coefficients

77 in reported cases between all pairwise municipality combinations confirm this ob-  
 78 servation (Figure 2B). In 830 out of 861 municipality combinations, correlation in  
 79  $\mathcal{R}(t)$  is higher than correlation in cases. This is reflected in the spatial synchrony  
 80 function for  $\mathcal{R}(t)$  (Figure 2C), where the mean cross-correlation for  $\mathcal{R}(t)$  ( $\rho = 0.71$ )  
 81 is considerably higher than that for cases ( $\rho = 0.30$ ).

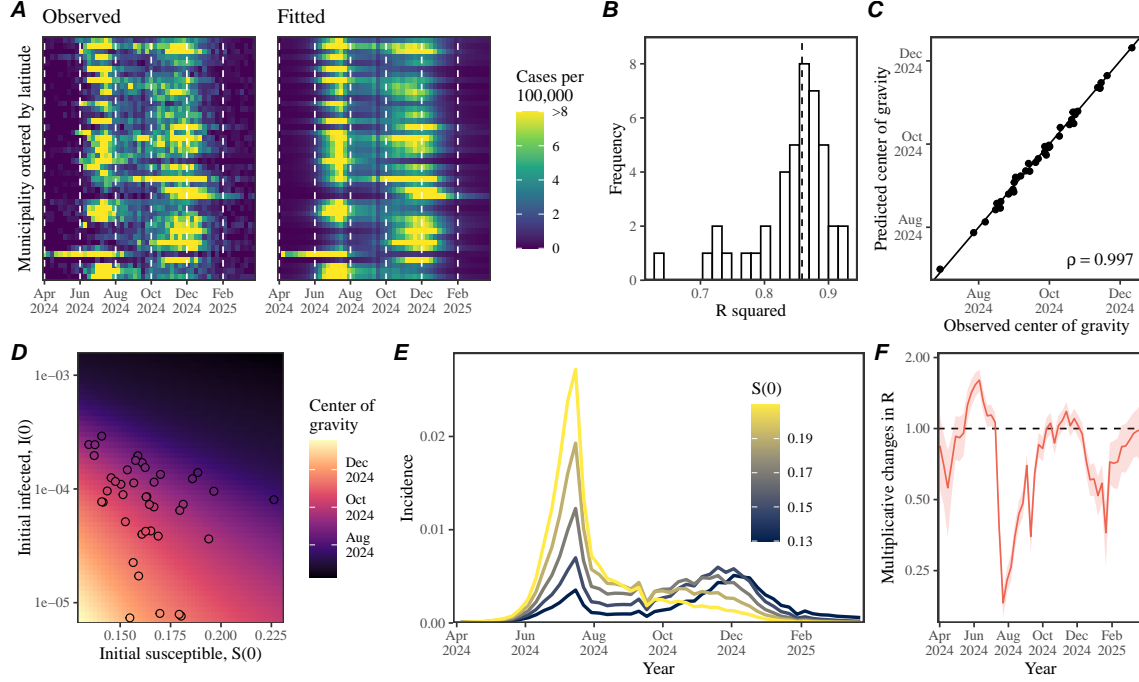


Figure 3: **Fine-scale spatiotemporal variation in pertussis epidemic can be explained with a simple SEIR model.** (A) Comparisons between the observed and predicted epidemic dynamics across municipalities with more than 400 total cases, ordered by latitude.. (B) The bar plot represents the distribution of  $R$  squared values for model fits. The vertical dashed line represents the median. (C) Relationship between the estimated and predicted center of gravity. The solid line indicated the one-to-one relationship. (D) Relationship between the initial susceptible  $S(0)$  and infected  $I(0)$  fraction with center of gravity. Points represent the estimates for each municipality. (E) Impact of initial susceptibility on pertussis epidemic dynamics. (F) Estimated time-varying pertussis transmission rate. The red line and shaded regions represent the posterior median and the corresponding 95% credible interval.

82 To better understand factors driving changes in  $\mathcal{R}(t)$ , we perform a regression  
 83 analysis using a generalized additive model with three covariates [17, 18, 19]: (1)  
 84 a municipality-level fixed effect allowing each municipality to have its own inter-  
 85 cept; (2) a cumulative-cases term capturing the effect of susceptible depletion; and  
 86 (3) a single smooth term shared across municipalities, which allows for temporal  
 87 changes in pertussis transmission over time, such as seasonal forcing. First, the

smooth term suggests a strong transmission reduction around August and February, which coincide with the timing of school breaks (Figure 2D). Second, the model estimates a significant effect of effect of susceptible depletion (Figure 2D;  $p < 0.001$ ). Notably, this simple regression model explains 84% of variance in  $\mathcal{R}(t)$ , suggesting that the observed temporal fluctuations in transmission can be largely explained by school-related seasonality and the gradual depletion of susceptible individuals. Taken together, the analysis of center of gravity and  $\mathcal{R}(t)$  suggest that differences in introduction timing and susceptible host dynamics are likely main drivers for spatial asynchrony in pertussis epidemics in Korea, rather than variation in seasonal transmission patterns.

## Mathematical modeling of fine-scale spatio-temporal pertussis epidemic

To test whether variation in introduction timing and susceptible dynamics alone can explain the observed epidemic patterns, we extended a standard susceptible-exposed-infected-removed (SEIR) model [20] to jointly estimated a single, time-varying transmission term, which is shared across all regions. We also allowed spatial variation in initial susceptible  $S(0)$  and infected  $I(0)$  fraction as well as the reporting rate  $\rho$ . Variation in  $S(0)$  captures differences in population-level susceptibility, whereas variation in  $I(0)$  effectively captures differences in introduction timing. For this analysis, we also focus on municipalities with more than 400 total cases. The model is fitted using a Bayesian inference software rstan [21].

Our simple transmission model that assume shared transmission rate can capture fine-scale spatiotemporal variation of pertussis outbreak in Korea (Figure 3A) with a median R squared value of 0.86 (95% quantile: 0.71—0.91). Furthermore, we find a near-perfect correlation between the predicted and observed center of gravity (Figure 3C). So what factors determine the timing of epidemic, and therefore the center of gravity? We address this question by simulating our model between April 2024 and April 2025 across plausible ranges of  $S(0)$  and  $I(0)$ .

First, increasing  $I(0)$  leads to an earlier epidemic because it permits earlier introduction of the infection to the population (Figure 3D). This is consistent with our earlier observations (Figure 1F). Similarly, increasing  $S(0)$  also results in an earlier epidemic. This is because high levels of susceptibility allows for a large first wave, which prevents the second wave through the overcompensatory susceptible depletion (Figure 3E). Finally, we estimate that the large reduction in transmission around late July 2024 and late January 2025 allowed the occurrence of two distinct epidemic waves (Figure 3F). this estimated timing of transmission reduction is consistent with our estimates from the  $\mathcal{R}(t)$  analysis and coincide with the timing of school holidays in Korea.

We validate our model by taking the estimated transmission term and fitting the remaining parameters (i.e., initial infected, initial susceptible, and reporting probability) to data from the remaining 210 municipalities with less than 400 total cases

129 (Figure S2). While model predictions appear consistent with the observed patterns  
130 (Figure S2A), we estimate a lower value for the median R squared: 0.58 (95% quan-  
131 tile: 0.04–0.87; Figure S2B). Nonetheless, our analysis suggests that the majority of  
132 asynchrony in pertussis epidemics can be explained via the differences in introduction  
133 timing and initial susceptibility.

## 134 Summary

135 Understanding mechanisms that drive spatiotemporal variation in epidemic dynamics  
136 is a major aim for infectious disease dynamics and control [1, 2, 3, 4, 7, 8, 9] The large  
137 pertussis outbreaks in Korea that occurred between 2024 and 2025 presents a unique  
138 perspective on a fine-scale spatiotemporal asynchrony heterogeneity in epidemic dy-  
139 namics: some municipalities experienced two epidemic waves while other places ex-  
140 perienced only the first or second without a clear patterns of synchrony. We propose  
141 that this variation can be explained by the differences in introduction delays and  
142 initial susceptibility, where high levels of susceptibility can cause a large first wave  
143 and prevent the second wave through susceptible depletion. Incorporating this idea  
144 into a simple transmission model by allowing for a joint estimation of a single trans-  
145 mission rate with variation in initial epidemic conditions confirms our hypothesis.  
146 Together, these findings demonstrate that differences in initial epidemic conditions—  
147 rather than variation in transmission—can generate fine-scale asynchrony, offering  
148 a general framework for understanding the spatiotemporal dynamics of re-emerging  
149 infections.

## 150 Caveats and future directions

151 Even though our model explains the observed dynamics reasonably well, there are  
152 several limitations to our work. First, our model is purely deterministic and does not  
153 account for stochasticity, which is likely an important factor for characterizing the  
154 establishment of infections after the initial invasion and the subsequent dynamics,  
155 especially in small populations [22, 23, 24]. Second, we estimated that a variation  
156 in susceptibility can explain the observed epidemic patterns, but we were unable to  
157 identify the mechanism that explains this variation. For example, we hypothesized  
158 that past vaccine coverage would explain variation in susceptibility given the role of  
159 waning immunity in driving pertussis re-emergence [25, 26, 27], but we did not find  
160 a significant correlation (Figure S3).

161 Our parameter estimates must be interpreted with care as our model relies on  
162 several simplifying assumptions. For example, we assumed the same values of basic  
163 reproduction number  $\mathcal{R}_0$  across all municipalities. Therefore, any regional variation  
164 in  $\mathcal{R}_0$ , driven by differences in contact rates and age distributions would be captured  
165 in our estimate of the initial susceptible fraction. In other words, our estimated  
166 susceptible fraction should be interpreted as the effective susceptibility that also

167 captures behavioral and sociological factors, beyond immunological differences. We  
168 also did not consider an age structure in our model, but age-structured contact  
169 patterns play an important role in shaping pertussis transmission [20]. For example,  
170 [28] recently suggested transmission among elderly may contributed to the persistence  
171 of pertussis in Korea. Despite these limitations, our work provides a quantitative  
172 foundation and empirical evidence for understanding epidemic asynchrony.

## 173 Conclusion

174 The continued emergence of new pathogens and re-emergence of vaccine preventable  
175 infections, such as pertussis, highlights the importance of identifying hotspots of  
176 future outbreaks and developing targeted intervention strategies [29, 30, 31]. The  
177 apparent asynchrony in pertussis epidemic in Korea, driven by the differences in in-  
178 troduction timing and population-level susceptibility, underlines the importance of  
179 detailed pathogen surveillance for early detection and strategic allocation of preven-  
180 tion and control resources.. Immunological surveillance platforms will be particularly  
181 useful for evaluating potential risk of pathogen re-emergence in the future [32, 33].  
182 A detailed understanding of spatial variation in population-level immunity will be  
183 crucial for predicting spatiotemporal dynamics of future outbreaks.

## 184 References

- 185 [1] Virginia E Pitzer, Cécile Viboud, Wladimir J Alonso, Tanya Wilcox, C Jessica  
186 Metcalf, Claudia A Steiner, Amber K Haynes, and Bryan T Grenfell. Environmental  
187 drivers of the spatiotemporal dynamics of respiratory syncytial virus in  
188 the United States. *PLoS pathogens*, 11(1):e1004591, 2015.
- 189 [2] Benjamin D Dalziel, Stephen Kissler, Julia R Gog, Cecile Viboud, Ottar N  
190 Bjørnstad, C Jessica E Metcalf, and Bryan T Grenfell. Urbanization and humidity  
191 shape the intensity of influenza epidemics in US cities. *Science*, 362(6410):75–  
192 79, 2018.
- 193 [3] Margarita Pons-Salort, M Steven Oberste, Mark A Pallansch, Glen R Abedi,  
194 Saki Takahashi, Bryan T Grenfell, and Nicholas C Grassly. The seasonality of  
195 nonpolio enteroviruses in the united states: Patterns and drivers. *Proceedings  
of the National Academy of Sciences*, 115(12):3078–3083, 2018.
- 197 [4] Rachel E Baker, Ayesha S Mahmud, Caroline E Wagner, Wenchang Yang, Vir-  
198 ginia E Pitzer, Cecile Viboud, Gabriel A Vecchi, C Jessica E Metcalf, and  
199 Bryan T Grenfell. Epidemic dynamics of respiratory syncytial virus in current  
200 and future climates. *Nature communications*, 10(1):5512, 2019.
- 201 [5] Michael P Hassell, Hugh N Comins, and Robert M Mayt. Spatial structure and  
202 chaos in insect population dynamics. *Nature*, 353(6341):255–258, 1991.

- 203 [6] JA Sherratt. Periodic travelling waves in cyclic predator–prey systems. *Ecology Letters*, 4(1):30–37, 2001.
- 204
- 205 [7] Bryan T Grenfell, Ottar N Bjørnstad, and Jens Kappey. Travelling waves and  
206 spatial hierarchies in measles epidemics. *Nature*, 414(6865):716–723, 2001.
- 207
- 208 [8] Derek AT Cummings, Rafael A Irizarry, Norden E Huang, Timothy P Endy,  
209 Ananda Nisalak, Kumnuan Ungchusak, and Donald S Burke. Travelling waves in  
210 the occurrence of dengue haemorrhagic fever in thailand. *Nature*, 427(6972):344–  
347, 2004.
- 211
- 212 [9] Cécile Viboud, Ottar N Bjørnstad, David L Smith, Lone Simonsen, Mark A  
213 Miller, and Bryan T Grenfell. Synchrony, waves, and spatial hierarchies in the  
spread of influenza. *science*, 312(5772):447–451, 2006.
- 214
- 215 [10] Robert S Paton, Christopher E Overton, and Thomas Ward. The rapid replace-  
216 ment of the SARS-CoV-2 Delta variant by Omicron (B. 1.1. 529) in England.  
*Science Translational Medicine*, 14(652):eab05395, 2022.
- 217
- 218 [11] Hye-Jin Kim, Young Joon Park, Dongkeun Kim, Jihee Lee, Yun Kyoung  
219 Kim, Soonryu Seo, Jin Seon Yang, Yeoeun Yun, Eunbyeol Wang, Subin Park,  
220 Seo Yeon Ko, Jin Lee, Jeeyeon Shin, Wookeon Lee, and Seonhee Ahn. Pertussis  
221 surveillance and occurrence report in the Republic of Korea: from 2024 to the  
first half of 2025. *Public Health Weekly Report*, 18(43):1631–1651, 11 2025.
- 222
- 223 [12] Hyun Mi Kang, Taek-Jin Lee, Su Eun Park, and Soo-Han Choi. Pertussis in  
224 the post-COVID-19 era: resurgence, diagnosis, and management. *Infection &  
Chemotherapy*, 57(1):13, 2024.
- 225
- 226 [13] Scott M Duke-Sylvester, Luca Bolzoni, and Leslie A Real. Strong seasonality  
227 produces spatial asynchrony in the outbreak of infectious diseases. *Journal of  
the Royal Society Interface*, 8(59):817–825, 2011.
- 228
- 229 [14] Marc Choisy and Pejman Rohani. Changing spatial epidemiology of pertussis  
230 in continental USA. *Proceedings of the Royal Society B: Biological Sciences*,  
279(1747):4574–4581, 2012.
- 231
- 232 [15] Jacco Wallinga and Marc Lipsitch. How generation intervals shape the relation-  
233 ship between growth rates and reproductive numbers. *Proceedings of the Royal  
Society B: Biological Sciences*, 274(1609):599–604, 2007.
- 234
- 235 [16] Anne Cori, Neil M Ferguson, Christophe Fraser, and Simon Cauchemez. A new  
236 framework and software to estimate time-varying reproduction numbers during  
epidemics. *American journal of epidemiology*, 178(9):1505–1512, 2013.

- 237 [17] Dennis E te Beest, Michiel van Boven, Mariëtte Hooiveld, Carline van den Dool,  
238 and Jacco Wallinga. Driving factors of influenza transmission in the netherlands.  
239 *American journal of epidemiology*, 178(9):1469–1477, 2013.
- 240 [18] Simon N Wood. *Generalized additive models: an introduction with R*. Chapman  
241 and Hall/CRC, 2017.
- 242 [19] Stephen M Kissler, Christine Tedijanto, Edward Goldstein, Yonatan H Grad,  
243 and Marc Lipsitch. Projecting the transmission dynamics of SARS-CoV-2  
244 through the postpandemic period. *Science*, 368(6493):860–868, 2020.
- 245 [20] Pejman Rohani, Xue Zhong, and Aaron A King. Contact network structure  
246 explains the changing epidemiology of pertussis. *Science*, 330(6006):982–985,  
247 2010.
- 248 [21] Bob Carpenter, Andrew Gelman, Matthew D Hoffman, Daniel Lee, Ben  
249 Goodrich, Michael Betancourt, Marcus Brubaker, Jiqiang Guo, Peter Li, and  
250 Allen Riddell. Stan: A probabilistic programming language. *Journal of statis-*  
251 *tical software*, 76:1–32, 2017.
- 252 [22] Bärbel F Finkenstädt, Ottar N Bjørnstad, and Bryan T Grenfell. A stochastic  
253 model for extinction and recurrence of epidemics: estimation and inference for  
254 measles outbreaks. *Biostatistics*, 3(4):493–510, 2002.
- 255 [23] James O Lloyd-Smith, Sebastian J Schreiber, P Ekkehard Kopp, and Wayne M  
256 Getz. Superspreading and the effect of individual variation on disease emergence.  
257 *Nature*, 438(7066):355–359, 2005.
- 258 [24] FMG Magpantay, M Domenech De Cellés, P Rohani, and AA King. Pertussis  
259 immunity and epidemiology: mode and duration of vaccine-induced immunity.  
260 *Parasitology*, 143(7):835–849, 2016.
- 261 [25] Helen J Wearing and Pejman Rohani. Estimating the duration of pertussis  
262 immunity using epidemiological signatures. *PLoS pathogens*, 5(10):e1000647,  
263 2009.
- 264 [26] Tina Tan, Tine Dalby, Kevin Forsyth, Scott A Halperin, Ulrich Heininger,  
265 Daniela Hozbor, Stanley Plotkin, Rolando Ulloa-Gutierrez, and Carl  
266 Heinz Wirsing Von König. Pertussis across the globe: recent epidemiologic  
267 trends from 2000 to 2013. *The Pediatric infectious disease journal*, 34(9):e222–  
268 e232, 2015.
- 269 [27] Matthieu Domenech de Cellès, Felicia MG Magpantay, Aaron A King, and Pej-  
270 man Rohani. The impact of past vaccination coverage and immunity on pertussis  
271 resurgence. *Science translational medicine*, 10(434):eaaj1748, 2018.

- 272 [28] Seonghui Cho, Dong Wook Kim, Chiara Achangwa, Junseo Oh, and Sukhyun  
273 Ryu. Pertussis in the elderly: Plausible amplifiers of persistent community  
274 transmission of pertussis in South Korea. *Journal of Infection*, 89(3), 2024.
- 275 [29] David L Heymann and Guénaël R Rodier. Hot spots in a wired world: Who  
276 surveillance of emerging and re-emerging infectious diseases. *The Lancet infectious  
277 diseases*, 1(5):345–353, 2001.
- 278 [30] Mahmoud M Naguib, Patrik Ellström, Josef D Järhult, Åke Lundkvist, and  
279 Björn Olsen. Towards pandemic preparedness beyond COVID-19. *The Lancet Microbe*,  
280 1(5):e185–e186, 2020.
- 281 [31] Hai Nguyen-Tran, Sang Woo Park, Kevin Messacar, Samuel R Dominguez,  
282 Matthew R Vogt, Sallie Permar, Perdita Permaul, Michelle Hernandez, Daniel C  
283 Douek, Adrian B McDermott, et al. Enterovirus D68: a test case for the use of  
284 immunological surveillance to develop tools to mitigate the pandemic potential  
285 of emerging pathogens. *The Lancet Microbe*, 3(2):e83–e85, 2022.
- 286 [32] Michael J Mina, C Jessica E Metcalf, Adrian B McDermott, Daniel C Douek,  
287 Jeremy Farrar, and Bryan T Grenfell. A global immunological observatory to  
288 meet a time of pandemics. *Elife*, 9:e58989, 2020.
- 289 [33] Hai Nguyen-Tran, Sang Woo Park, Matthew R Vogt, Perdita Permaul, Alicen B  
290 Spaulding, Michelle L Hernandez, Jennifer A Bohl, Sucheta Godbole, Tracy J  
291 Ruckwardt, Peter W Krug, et al. Dynamics of endemic virus re-emergence in  
292 children in the USA following the COVID-19 pandemic (2022–23): A prospective,  
293 multicentre, longitudinal, immunoepidemiological surveillance study. *The Lancet Infectious Diseases*.